Physics of the Solid State, Vol. 46, No. 8, 2004, pp. 1528–1532. Translated from Fizika Tverdogo Tela, Vol. 46, No. 8, 2004, pp. 1484–1488.

LOW-DIMENSIONAL SYSTEMS AND SURFACE PHYSICS

Analysis of Raman Spectra of Amorphous–Nanocrystalline Silicon Films

S. V. Gaĭsler*, O. I. Semenova, R. G. Sharafutdinov***, and B. A. Kolesov******

**Novosibirsk State University, ul. Pirogova 2, Novosibirsk, 630090 Russia*

***Institute of Semiconductor Physics, Siberian Division, Russian Academy of Sciences, pr. Akademika Lavrent'eva 13, Novosibirsk, 630090 Russia*

****Institute of Thermal Physics, Siberian Division, Russian Academy of Sciences, pr. Akademika Lavrent'eva 1, Novosibirsk, 630090 Russia*

*****Nikolaev Institute of Inorganic Chemistry, Siberian Division, Russian Academy of Sciences, pr. Akademika Lavrent'eva 3, Novosibirsk, 630090 Russia*

e-mail: kolesov@che.nsk.su

Received October 30, 2003

Abstract—A new method is proposed for the treatment of Raman spectra of amorphous–nanocrystalline silicon films serving as a major component in solar cells. The method is based on the well-known theory of strong spatial localization (confinement) of phonons and offers the possibility of estimating the fractional content of the amorphous and crystalline phases in a film and the size distribution of nanocrystals. © *2004 MAIK "Nauka/Interperiodica".*

1. INTRODUCTION

Interest in photoelectric solar power converters stems from ecological considerations and the steady reduction of their production costs, which makes them the most promising source of renewable energy. The efforts of researchers and engineers working in the area of solar cell production have been shifting increasingly toward the development of thin-film silicon technology. Deposition of amorphous and microcrystalline silicon layers on low-cost substrates (stainless steel, plastics, glass) appears presently to hold the greatest promise [1–3]. Films prepared in these conditions are usually a mixture of amorphous and microcrystalline silicon. The crystalline phase consists, as a rule, of nanocrystals 30–100 Å in size differing from bulk crystals in terms of their physical properties. The characteristics of thin-film solar cells are governed to a considerable extent by the properties of the silicon layers, which makes monitoring their physical characteristics and phase composition an aspect of paramount importance. Raman spectroscopy is the most appropriate and convenient method for reaching this goal due to its high speed (the time required to measure the spectrum of a Si film is ≈1 min), high spatial resolution (1–2 μm), nondestructive character, and the fact that there is no need for preliminary sample preparation. The spectrum contains complete information on the phase composition of the sample, and the problem actually consists in extracting this information as fully as possible.

The phonon spectrum of nanocrystals is usually described in terms of the model proposed in [4, 5] postulating strong spatial localization (confinement). Assuming spherical crystallites of diameter D and phonon decay following the $\exp(-\alpha r^2 D^2)$ law, the Raman line shape is given by the integral [5]

$$I(\omega) \propto \int \exp\left(-\frac{q^2 D^2}{4}\right) \frac{d\mathbf{q}}{[\omega(\mathbf{q}) - \omega]^2 + (\Gamma_0/2)^2}, \quad (1)$$

where Γ_0 is the natural linewidth of a bulk crystal and $\omega(\mathbf{q})$ is the phonon frequency. The phonon wave vector is expressed in units of $2\pi/a_0$, where a_0 is the silicon lattice constant (0.543 nm).

This expression was employed in [6] to describe an experimental Raman spectrum of a film assuming it to consist of crystallites of one size and the amorphous phase. In analyzing the Raman spectra of porous silicon, the problem was complicated in [7] by assuming a Gaussian size distribution of crystallites and by introducing the corresponding factor into integral (1).

In [8], the ratio between the scattering intensities at frequencies of 520 cm^{-1} (I_c) and 480 cm^{-1} (I_a) in the film spectrum was accepted as a measure of sample crystallinity. Being straightforward and simple to obtain, the I_c/I_a ratio is essentially an abstract parameter that is in no way related to the real film structure. For this reason, the content of the crystalline phase was additionally determined in [8] by deconvoluting the spectrum into four components, two of which corresponded to the amorphous phase and the other two, to crystallites 35 and 200 Å in size.

This communication pursues a somewhat different goal. We believed it essential to estimate this distribution from the spectra themselves, rather than to preset

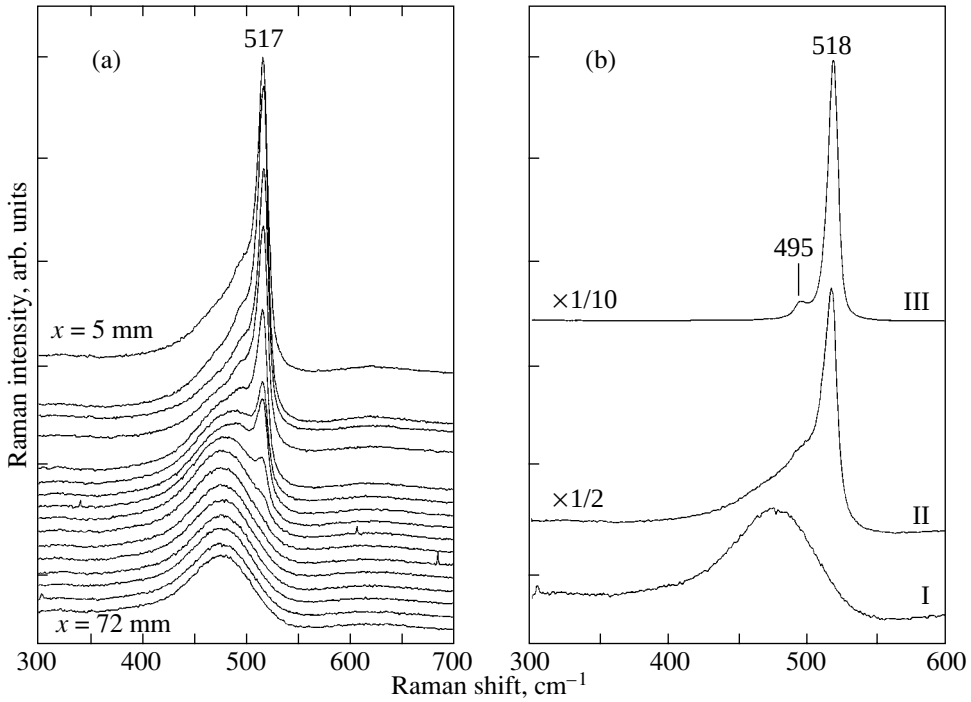

Fig. 1. (a) Raman spectra obtained from different regions of the same silicon film at different distances from its edge and (b) typical Raman spectra of films. Intensity of spectrum II is halved (×1/2), and that of spectrum III is reduced by ten times (×1/10).

the nanoparticle size distribution in advance in analyzing various Raman spectra of amorphous–nanocrystalline silicon films. Our approach would enable one to extract as fully as possible the information contained in a spectrum and to correct the technological conditions of film deposition.

2. EXPERIMENTAL

The amorphous–nanocrystalline silicon films under study were prepared using the gas-jet electron-beam plasma-enhanced chemical vapor deposition technology (GJEB PE CVD) [9]. The film thickness was derived from reflectance spectra in the near IR region (800–2000 nm, UV 3101PC spectrophotometer, Shimadzu) and varied within 300–600 nm.

Raman spectra were measured with a Triplemate SPEX spectrometer equipped with a liquid nitrogen–cooled LN 1340PB (Princeton Instruments) multichannel CCD camera. The spectra were excited by a 488-nm argon laser line with a power at the sample surface of no greater than 5 mW. The excitation wavelength was chosen so as to reduce the light penetration depth and prevent formation of the substrate spectrum, and the excitation power was low in order to preclude light-induced sample crystallization. The sample was placed in the focal plane of a microscope whose objective, (LD EPIPLAN, 40/0.60 Pol. Zeiss), with an operating distance of 2 mm and an aperture of 0.6, served to focus the laser beam and collect the scattered radiation. The laser beam spot on the sample surface was 2 μm in diameter. In the experiments, 180° scattering geometry was used. Raman spectra of films were measured with a resolution of 5 cm^{-1}.

3. RESULTS

Figure 1a presents Raman spectra of a film obtained for different values of the distance x (in mm) from the edge of the film facing the nozzle of the gas source, and Fig. 1b shows typical Raman spectra, two of which (I, II) are those shown in Fig. 1a and the third (III) was measured on a film prepared in different technological conditions.

One readily sees that Raman spectra reflect either solely an amorphous state with a broad band peaking at ~475 cm^{-1} (Fig. 1b, I), an amorphous–nanocrystalline state (Fig. 1b, II), or again a predominantly nanocrystalline phase (Fig. 1b, III). The Raman band peak position of nanoparticles varies from 514 to 518 cm^{-1}; i.e., it is always lower than the phonon frequency in a bulk crystal (520 cm^{-1}). Note the feature at 495 cm^{-1} in spectra II and III (Fig. 1b), whose origin still remains to be established.

4. ANALYSIS OF THE RAMAN SPECTRA

To describe the structure of a film, namely, the degree of its crystallinity and the nanocrystal size distribution, we introduce a trial function. To do this, we use Eq. (1) to calculate the line profiles for nanocrystals

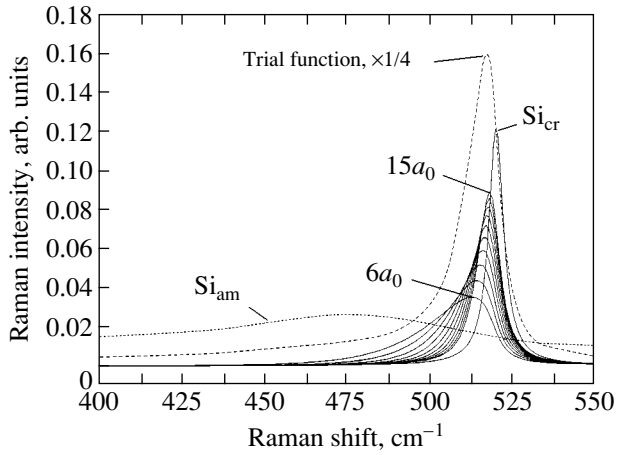

Fig. 2. Calculated profiles of Raman spectra from particles with different diameters (solid lines) and from the amorphous phase. All spectra are normalized against unit integrated intensity. Dashed line is a trial function (see text). The intensity for the trial function is reduced by four times (×1/4).

with a diameter of $6a_0$ (3.3 nm), $7a_0$, etc., up to $15a_0$ and assign the same integrated intensity of unity to each line. The lower limit corresponds to particles ~3 nm in diameter, and the upper limit, to ~8 nm. Identification of particles less than 3 nm in diameter with crystalline formations is questionable. The profiles calculated for nanocrystals with diameters above $15a_0$ are close to one another and to the spectrum of a bulk crystal in terms of peak position and halfwidth and thus can be replaced by the latter. The spectrum of crystalline silicon obtained under the same conditions as the spectra of the other samples has a Lorentzian profile centered at 520 cm^{-1} with a halfwidth of 6 cm^{-1}. The calculated profiles are presented in Fig. 2. Also shown is a band corresponding to the amorphous phase, likewise with a unit intensity, and representing not a calculated Gaussian or a Lorentzian profile but rather an envelope of an experimental spectrum of a pure amorphous phase (bottom spectrum in Fig. 1a) intended to take into account the scattering from acoustic phonons and second-order scattering from combination tones. The amorphous and the nanocrystalline components are normalized in the same way, which finds justification in the fact that the integrated intensities (scattering cross sections) of both components are similar, $I_c/I_a = 0.95$ [6]. (In actuality, the integrated Raman line intensity of a crystal is about seven times that of the amorphous phase, which should be assigned to a difference not in the scattering cross section but rather in the absorption coefficient and, accordingly, in the depth of exciting-light penetration into the sample.) Summing up all the profiles, we obtain a trial function (Fig. 2). The contribution of each component to the experimental spectrum can be estimated by reduction, i.e., by mathematically dividing the experimental spectrum by a trial function. Figure 3a illustrates the reduction of typical spectra I, II, and III from Fig. 1b. Each of the spectra gives an idea of the phase contents and the distribution of particles in size. Because each of the spectra contains a large fraction of the amorphous phase (100% for spectrum I), one can make them still more revealing by subtracting spectrum I

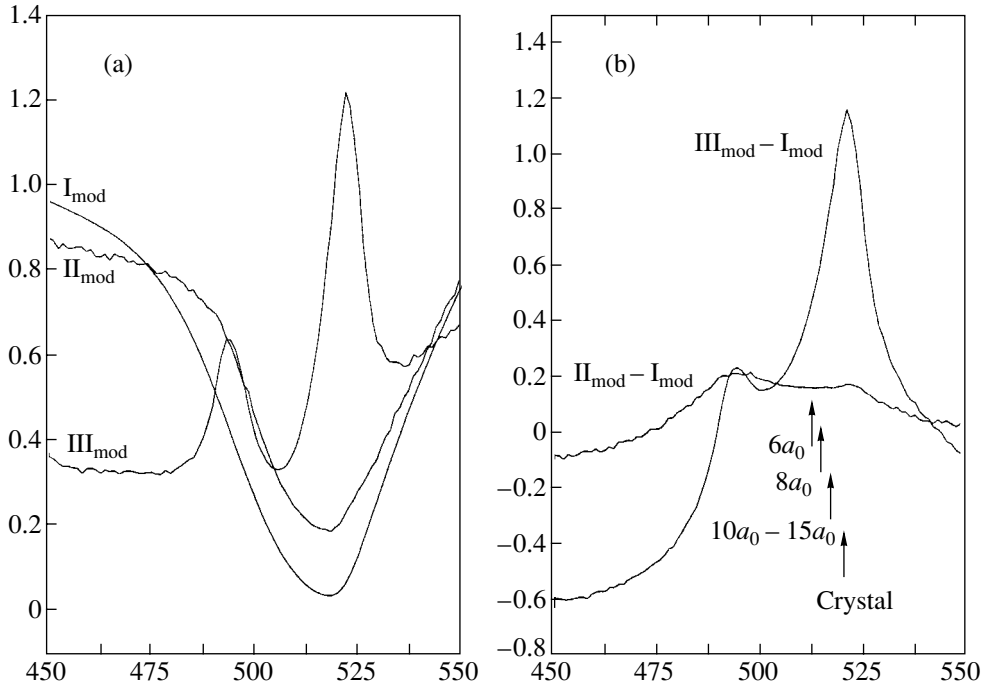

Fig. 3. (a) Reduction of the typical Raman spectra presented in Fig. 1b and (b) the difference between the reduced spectra (see text).

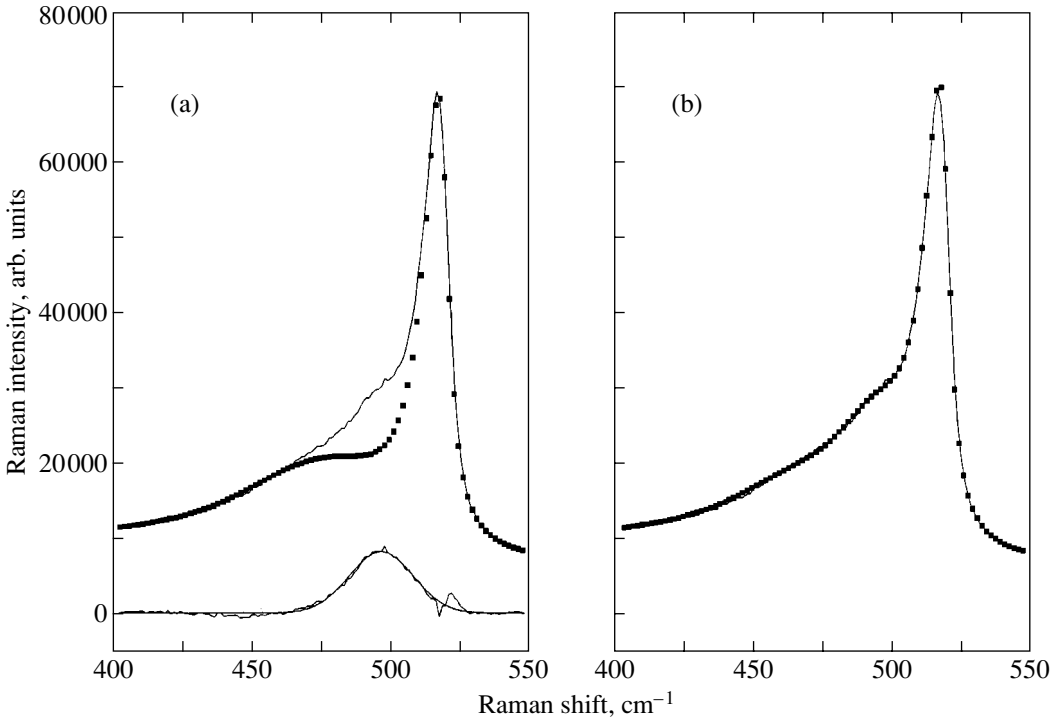

Fig. 4. (a) Comparison of the reconstructed Raman spectrum (without scattering at the *L* point) with the experimental spectrum (above), and the difference between the experimental and calculated spectra (below). (b) Same with scattering at the *L* point added. Solid line is experiment, and points are calculation.

from spectra II and III. The result of this procedure is displayed in Fig. 3b. Of most interest is the reduction of spectrum II, because spectra of this type are frequently met in studies of films and are the most difficult to interpret. As is evident from the distributions in Fig. 3, the fraction of the amorphous phase in the sample characterized by spectrum II is ~90%. The size distribution of nanoparticles is practically uniform, with a very weakly pronounced decrease in the fraction of large particles and of the bulk crystal. This may be used as a basis to attempt to reconstruct the experimental spectrum by adding up the corresponding fractions of "single-particle" functions and the amorphous phase (Fig. 2). The sum of the Raman spectra of nine fractions of the amorphous phase, particles $7a_0$, $8a_0$, …$14a_0$ in size (one fraction for each size), a 1/2 fraction of particles $15a_0$ in size, and a 1/4 fraction of the crystalline phase (i.e., of all nanoparticles more than 8 nm in size) is presented in Fig. 4a. We readily see that the reconstructed Raman spectrum is in accord with experiment in the frequency region corresponding to the amorphous phase and nanocrystals but disagrees with the experimental spectrum in the intermediate region 490–500 cm^{-1}. The application of scattering profiles to particles $6a_0$ or less in diameter, which have a strong and extended low-frequency wing, results in a considerable deviation of the calculated spectrum from the experimental spectrum in the range 400–480 cm^{-1}. The difference between the two spectra (Fig. 4a, bottom) is a Gaussian centered at 496 cm^{-1} with a halfwidth of 23 cm^{-1}. A similar feature, but shaped as a well-resolved spectral band, becomes manifest in the sample with a large (~60%) content of the nanocrystalline phase (spectrum III in Fig. 1b). It is well known that, at the center of the Brillouin zone of silicon, there may be one threefold degenerate vibration mode F_{2g}, which includes two transverse and one longitudinal optical phonon. When moving along the dispersion curve toward one of the high-symmetry points, this vibration splits into the TO and LO modes, whose frequencies at the *L* point are 493 and ~400 cm^{-1}, respectively [10]. Thus, the TO(*L*)-phonon frequency practically coincides with the position of the feature observed in the Raman spectra of films (495 cm^{-1} for the line in spectrum III in Fig. 1b). First-order Raman scattering at the zone-edge critical points is forbidden, but in nanocrystals the wave-vector selection rules are violated because of the decrease in the phonon correlation length, thus making such scattering possible. The same effect is responsible for the detection of frequency-shifted localized phonon modes at the zone center in nanocrystals. The phonon density of states and the vibration frequencies at the critical points in silicon have been repeatedly studied both theoretically and experimentally (see, e.g., [11]).

Figure 4b presents an experimental and a reconstructed spectrum with inclusion of the scattering at the *L* point. In this case, the agreement between the two spectra is quite satisfactory.

To sum up, Raman spectra contain complete information on the phase composition and structure of amorphous–crystalline films, which can be extracted through special treatment of the spectral data.

ACKNOWLEDGMENTS

The authors are deeply indebted to V.A. Gaĭsler (ISP, SD RAS) for useful discussions and valuable comments.

This study was supported by INTAS, project no. 01-2257.

REFERENCES

1. K. R. Catchpole, M. J. McCann, K. J. Weber, and A. W. Blakers, Sol. Energy Mater. Sol. Cells **68** (2), 173 (2001).
2. Yoshihiro Hamakawa, Sol. Energy Mater. Sol. Cells **74** (1), 13 (2002).
3. R. B. Bergmann and J. H. Werner, Thin Solid Films **403–404**, 162 (2002).
4. H. Richter, Z. P. Wang, and L. Ley, Solid State Commun. **39** (5), 625 (1981).
5. L. H. Campbell and P. M. Fauchet, Solid State Commun. **58** (10), 739 (1986).
6. V. G. Golubev, V. Yu. Davydov, A. V. Medvedev, A. B. Pevtsov, and N. A. Feoktistov, Fiz. Tverd. Tela (St. Petersburg) **39** (8), 1348 (1997) [Phys. Solid State **39**, 1197 (1997)].
7. Md. N. Islam and K. Satyendra, Appl. Phys. Lett. **78** (6), 715 (2001).
8. T. Kamei, P. Stradins, and A. Matsuda, Appl. Phys. Lett. **74** (12), 1707 (1999).
9. R. Sharafutdinov, S. Khmel, O. Semenova, S. Svitasheva, R. Bilyalov, and J. Poortmans, in *Proceedings of the 29th IEEE Photovoltaic Specialists Conference, New Orleans, USA, 2002* (IEEE, New York, 2002), p. 1178.
10. M. Balkanski and M. Nusimovici, Phys. Status Solidi **5**, 635 (1964).
11. M. Cardona, in *Light Scattering in Solids*, Ed. by M. Cardona and G. Guntherodt, 2nd ed. (Springer, Berlin, 1982; Mir, Moscow, 1984), Vol. 2.

Translated by G. Skrebtsov